

Search for the $N(1685)$ in $\eta\pi$ -Photoproduction

Dominik Werthmüller^{1,*} on behalf of the A2 Collaboration at MAMI

¹Department of Physics, University of York, Heslington, York, YO10 5DD, UK

Abstract. The nucleon-like member $N(1685)$ of the speculative baryon antidecuplet denotes one possible explanation for the narrow peak-structure around $W = 1.68$ GeV observed in the total cross section of η -photoproduction off the neutron. If this baryon existed, it would likely to be seen in other reactions as well. While the aforementioned peak, whatever its nature is, was confirmed by several experiments, claims for signatures of the $N(1685)$ in other reactions and observables are mainly made by V. Kuznetsov *et al.* using GRAAL data. Their latest work suggests signals of both $N(1685)$ charge states in all isospin channels of $\eta\pi$ -photoproduction off the proton and neutron. This contribution reports on challenging these claims with data from the A2 at MAMI experiment employing photon beam energies from $E_\gamma=1.43\text{--}1.58$ GeV. The $\eta\pi^0 p$ and $\eta\pi^+ n$ final states produced from a hydrogen target were studied and new analysis cuts were tested in order to enhance a possible signal.

1 Introduction

The search for exotic states denotes a major focus of contemporary hadron physics. Such bound states of the strong interaction are not built from ordinary $q\bar{q}$ (for mesons) and qqq (for baryons) configurations in terms of the quark model but involve $q\bar{q}q\bar{q}$ (tetraquark), $qqqq\bar{q}$ (pentaquark), etc. as well as gluonic degrees of freedom to constitute a color singlet.

1.1 Exotic Pentaquarks

The most recent experimental evidence for pentaquark states was claimed in 2015 by the LHCb collaboration in the $J/\psi p$ final state of Λ_b^0 decays hinting at an $uudc\bar{c}$ quark content [1]. In the meantime, a total of three states are thought to be identified [2]. GlueX, a first independent experiment using J/ψ -photoproduction as an alternative production mechanism could not see any evidence of these pentaquark states [3]. More data from GlueX and other experiments are being taken and analyzed, and theoretical efforts to understand the production mechanisms are ongoing [4].

Before the evidence for pentaquarks containing heavy charm quarks emerged, in 2003 the LEPS collaboration claimed evidence for a $uudd\bar{s}$ pentaquark state named Θ^+ [5]. In the peculiar episode that followed the announcement, several experiments initially confirmed the existence of a structure around $W = 1540$ MeV in the KN system. In the end, however, large statistics measurements, mainly from the CLAS experiment, could not confirm the initial findings (see [6] for an overview). Nevertheless, as the detector acceptances of CLAS and LEPS are quite different, new LEPS results using an improved setup and analysis

are still awaited eagerly [7]. In addition, there are newer positive claims from the DIANA experiment [8] and a subgroup of the CLAS collaboration [9].

Pentaquark states were studied using the quark model long before the Θ^+ claim [10, 11]. The search for such a state at LEPS, although, was motivated by the striking prediction of the Chiral Quark-Soliton Model [12], a Skyrme model in which baryons are described as solitons of the chiral field. This model not only describes the known octet and decuplet but also predicts the antidecuplet depicted in figure 1. The exotic Z^+ (later renamed to Θ^+) with isospin $I = 0$ and strangeness $S = 1$ was predicted to be as narrow as 1 MeV and to decay into $K^+ n$ or $K^0 p$, which matched the LEPS results.

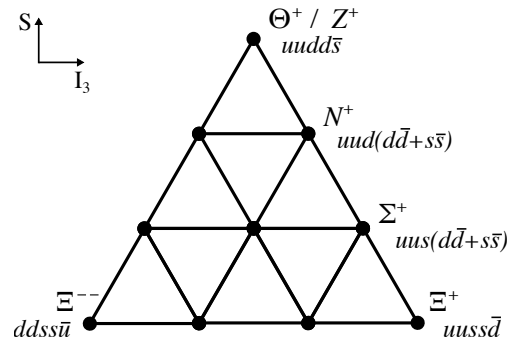


Figure 1. Antidecuplet $\overline{10}$ predicted by the Chiral Quark-Soliton Model [12].

1.2 The Cryptoexotic $N(1685)$

The nucleon-like antidecuplet state $N_{\overline{10}}$ was first identified with the nucleon resonance $N(1710)1/2^+$ (although

*e-mail: dominik.werthmueller@york.ac.uk

the width of the N_{10}^- was predicted to be much more narrow) in order to calculate the masses of the other members of the multiplet [12]. The N_{10}^- (as well as the Σ_{10}^-) is cryptoexotic, i.e., its quantum numbers can also be realized in an ordinary qqq configuration. It was quite a surprise when in 2007, Kuznetsov *et al.* (members of the GRAAL collaboration) presented evidence for a N_{10}^- candidate with matching properties [13]: The bump at $W = 1685$ MeV was observed in the cross section of η -photoproduction on the neutron in agreement with the leading $N_{10}^- \rightarrow \eta N$ decay [12]. Secondly, the width of the structure was very narrow (around 30 MeV) [14] compared to usual nucleon resonances. Thirdly, the absence of any bump in the corresponding cross section on the proton matched the predicted small photocoupling compared to the neutron (‘neutron anomaly’) [15].

While first there were doubts about the presence of the structure in the η -photoproduction cross section, the bump was observed by several independent experiments, such as LNS [16], CBELSA/TAPS [17, 18] and A2 at MAMI [19–21]. Similar structures are also claimed to be present in different reaction channels and observables, namely the beam asymmetry Σ in $\gamma p \rightarrow \eta p$ [22], and in Compton scattering off the neutron (cross section [23]) and off the proton (beam asymmetry Σ [24]). These results all originate from the GRAAL experiment and remain unconfirmed by any other experiment so far.

In view of some early analyses of the available data supporting the scenario of a new narrow resonance [14, 25–28], a $N(1685)$ with unknown quantum numbers was added as a one-star resonance to the 2012 Review of Particle Physics [29] by the Particle Data Group (PDG). The entry was removed in later editions when theoretical studies and partial-wave analyses showed that the bump around $W = 1685$ MeV in the η -photoproduction cross section on the neutron could also be due to coupled-channel effects of known nucleon resonances [30, 31], effects from strangeness threshold openings [32] and cusps [33], and S_{11} interferences [27, 34, 35]. More insight will be gained from the ongoing measurements of polarization observables, with first results for the observable E already available [36–38]. This work revealed that a calculation of the Bonn-Gatchina (BnGa) model [35] including a narrow P_{11} resonance gave a slightly better description of the experimental data than the model without a narrow state. Due to the limited statistics, the significance of this finding is still under debate [39].

1.3 Motivation for this work

The latest claim of a N_{10}^- signature as a narrow $N(1685)$ resonance is again made by Kuznetsov *et al.* using GRAAL data in the $\gamma N \rightarrow \eta \pi N$ channels [40]. Here, the N_{10}^- could be produced in the decay of a heavier N or Δ resonance R via the emission of a pion $R \rightarrow \pi N_{10}^-$ followed by the decay $N_{10}^- \rightarrow \eta N$. Therefore, in contrast to the direct production potentially observed in $\gamma n \rightarrow \eta n$, the signal could also be observed using a proton target despite the suppressed photon coupling of the N_{10}^- . Indeed, signals in all four isospin channels of $\gamma N \rightarrow \eta \pi N$ are claimed in

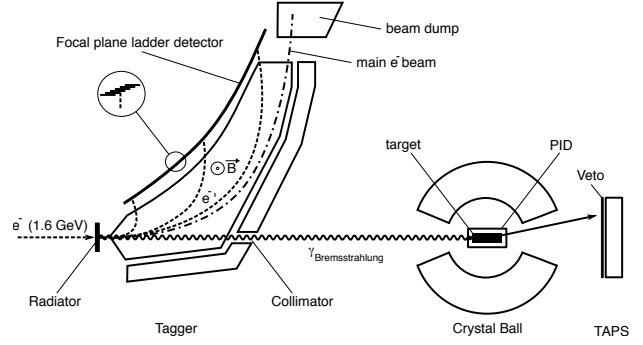


Figure 2. Schematic view of the setup at the tagged-photon beam experiment A2 at MAMI.

[40], whereas only the peak in $\gamma p \rightarrow \eta \pi^0 p$ (measured on the free proton) is statistically significant.

The $\gamma N \rightarrow \eta \pi N$ reactions have been previously measured at several experiments, such as LNS [41], GRAAL [42], CBELSA/TAPS [43–45] and A2 at MAMI [46–50]. The main findings were that for $E_\gamma < 1.6$ GeV, the reaction is dominated by the excitation of the $\Delta(1700)3/2^-$ and the $\Delta(1940)3/2^-$ resonances with subsequent decays to $\eta \Delta(1232)3/2^+$. Smaller contributions come from the $\pi N(1535)1/2^-$ isobar and photoproduction of the $a_0(980)$ meson. Evidence of a $N(1685)$ was not found in any of these studies as statistics was either limited or the event selection was not optimized to reveal a potential signal. The goal of this work is therefore to measure $\gamma p \rightarrow \eta \pi^0 p$ and $\gamma p \rightarrow \eta \pi^+ n$ in order to look for any signs of a narrow structure around $m(\eta N) \sim 1685$ MeV. The available A2 data for the energy range $E_\gamma = 1.43$ – 1.58 GeV have not been used so far to study these reactions.

2 Experimental Setup

The experimental data were obtained at the tagged-photon beam facility A2 at the electron-accelerator facility MAMI in Mainz, Germany. Out of three data sets of similar size, one data set of 310 hours was used for this work. Figure 2 shows an overview of the experimental setup. In contrast to ‘standard’ experiments, the Endpoint-Tagger (EPT) device allowing to access photon-beam energies $E_\gamma = 1.43$ – 1.58 GeV close to the energy of the incoming 1.6 GeV electron beam was installed. The 10-cm liquid hydrogen target was installed in the center of the Crystal Ball detector (CB) consisting of 672 NaI(Tl) crystals, which cover polar angles from 20–160 degrees with almost full azimuthal acceptance. Particles with polar angles from 5–20 degrees were detected in the TAPS calorimeter wall installed 1.5 m downstream from the target comprising 366 BaF₂ crystals. Thin plastic scintillator detectors arranged as a barrel around the target in CB and in front of individual TAPS crystals allowed charged-particle vetoing and particle identification via a dE/E -analysis in both calorimeters. Particles detected in TAPS could also be discriminated by time-of-flight and pulse-shape analyses, the latter utilizing the two scintillation-light components in the

BaF₂ crystals. The experimental trigger required an energy deposition higher than ~ 550 MeV in CB as the primary goal of the EPT-experiments were studies involving the η' -meson. More details about the setup can be found in [51].

3 Data Analysis

The following reactions were analyzed in this work:

- 1) $\gamma p \rightarrow \eta\pi^0 p$ with $\eta \rightarrow 2\gamma$
- 2) $\gamma p \rightarrow \eta\pi^+ n$ with $\eta \rightarrow 2\gamma$
- 3) $\gamma p \rightarrow \eta\pi^+ n$ with $\eta \rightarrow 3\pi^0 \rightarrow 6\gamma$

3.1 Event Selection

As for now, exclusive analyses were performed, i.e., all particles in the final state were required to be detected. The thresholds for clusters in the CB and TAPS calorimeters were set to 20 MeV. Using the detected particles, all combinations to form the corresponding final states were checked with a series of cuts. In addition, a kinematic fit was performed to optimize the measured angles and energies of the particles using 4-momentum and meson invariant-mass constraints. Particle identification was performed with dE/E (CB) and time-of-flight (TAPS) analyses for pion and neutron candidates in reactions 2) and 3). BaF₂ pulse-shape cuts were used in all reactions to separate photons from massive particles. Next, cuts on the reaction kinematics were implemented. Neutral pions and η -mesons were identified in the corresponding $m(\gamma\gamma)$ invariant masses by applying 3σ -cuts around their nominal mass. All particles were required to lie in the same reaction plane — this was ensured by cutting on the three azimuth-angle differences between the $p_i p_j$ and p_k systems ($p \in \{\eta, \pi, N\}$). A further cut was employed on the angular difference between the detected and fitted direction of the nucleon. The confidence level (CL) provided by the kinematic fit allowed an additional cut ($CL > 2.7 \times 10^{-3}$) to reject background events. Having applied all cuts, the number of events with multiple valid particle combinations were small. In order to account for them in the signal extraction, large data sets of Monte-Carlo (MC) simulations are needed. Therefore, for the current work only the combination with the highest CL was kept for further analysis.

3.2 Signal Extraction

The data were analyzed in bins of photon-beam energy E_γ and η -nucleon invariant mass $m(\eta N)$. In order to remove any background remaining after the previously discussed cuts, the $\eta\pi$ -missing mass (in case of reaction 1) and 2), nucleon mass subtracted) or the $m(3\pi^0)$ -invariant mass (in case of reaction 3)) were fitted with signal and background contributions obtained from MC simulations using a Geant4-based [52] model of the A2 experiment. The reason for the choice of different fit variables is the fact that very little background is present in analysis 3) and the $m(3\pi^0)$ -invariant mass provided more stable and

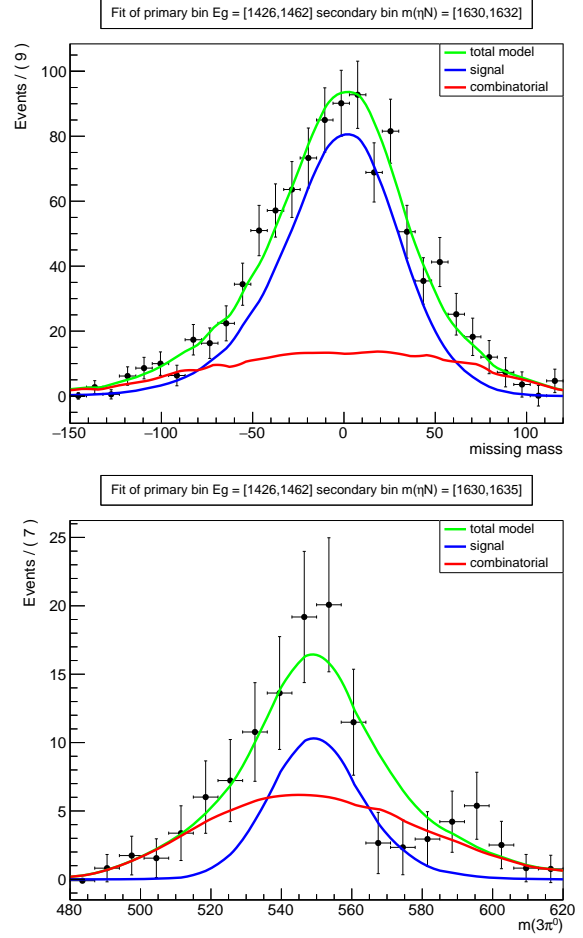


Figure 3. Example unbinned likelihood fits for the same E_γ , $m(\eta N)$ -bin. Top: Fit of the $\eta\pi^0$ -missing mass in the analysis of $\gamma p \rightarrow \eta\pi^0 p$ with $\eta \rightarrow 2\gamma$. Bottom: Fit of the $m(3\pi^0)$ -invariant mass in the analysis of $\gamma p \rightarrow \eta\pi^+ n$ with $\eta \rightarrow 3\pi^0$. Signal and background contributions were obtained from MC simulations.

unambiguous fits compared to the $\eta\pi$ -missing mass. Example fits of both types are shown in figure 3. Unbinned likelihood fits were performed which allowed to make use of the sPlot-technique [53] to obtain weights for the signal and background contribution on an event-by-event basis. This enables to unfold signal and background in any variable that is not correlated with the fit variable.

3.3 Van Hove Plots and Longitudinal Phase-Space

The use of longitudinal phase-space allows to reduce the phase-space dimensionality of multi-particle final states by assuming that the transverse momenta can be neglected in high-energy particle collisions [54]. In case of a three-particle final state, the longitudinal phase-space has two dimensions and Van Hove plots containing six sectors can be constructed. The sectors represent the possible combinations of the longitudinal momenta of all particles, i.e., whether they are going forward (direction of beam) or backward (direction of target) in the center-of-mass frame. As different reaction mechanisms will populate different

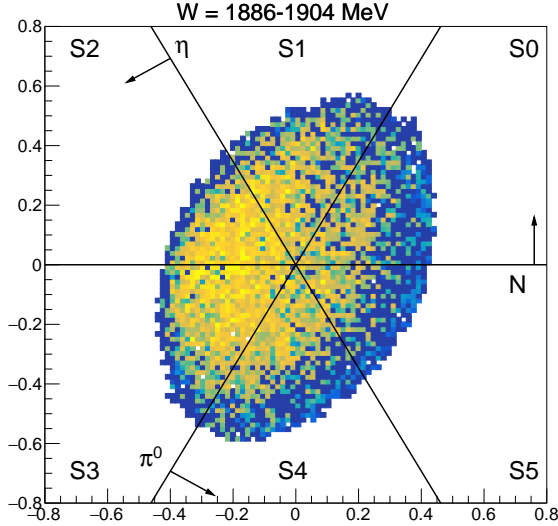


Figure 4. Van Hove plot for $\gamma p \rightarrow \eta \pi^0 p$ in the energy range $E_\gamma = 1426\text{--}1462$ MeV. The six sectors S0 to S5 represent different combinations of forward or backward going particles (see text).

sectors, Van Hove plots can be used to disentangle different processes.

The aim of the work performed here was to investigate the possibility of using Van Hove plots to separate the potential production of the $\pi N(1685)$ isobar from the dominating $\eta \Delta(1232)$ isobar. The main caveat is that in the studied energy range the transverse momenta cannot be neglected as required by the longitudinal phase-space approximation. Nevertheless, a partial separation could already lead to a sufficient improvement of the signal-to-background ratio.

Figure 4 shows the Van Hove plot for the first energy bin in the $\gamma p \rightarrow \eta \pi^0 p$ analysis. The sector with the largest number of events is S3, consistent with the dominating production of the $\eta \Delta(1232)$ isobar, with a forward going η -meson and $\pi^0 p$ going backward. Similarly, a possible $\pi N(1685)$ isobar is expected to be predominantly located in sector S5 assuming a production mechanism which yields a backward-going $N(1685)$ and a forward-going π -meson. As mentioned before, due to the relatively low beam energy, the loci for the different production mechanisms are not confined to one sector and strongly overlap.

4 Preliminary Results

Preliminary results of the observable of interest, the $m(\eta N)$ invariant mass, are shown in figures 5–8 and will be discussed in the following.

4.1 Uncut Distributions

First, the invariant mass distributions were studied using the standard analysis cuts discussed in section 3.1. In case of the $\gamma p \rightarrow \eta \pi^0 p$ reaction, the results shown in figure 5 are compared to the distributions obtained from phase-space MC simulations using event weights from the

BnGa partial-wave analysis of [45], which were scaled to the data using the ratio of the distribution integrals. No acceptance correction has been applied here. There is an overall good agreement between the two distributions with a small discrepancy at the maximum, where the data shows a slightly sharper shape. No excess around 1685 MeV is observed. Only the $\eta \rightarrow 2\gamma$ decay has been analyzed so far, as the $\eta \rightarrow 3\pi^0$ decay leads to a total number of nine particles in the final state, which will degrade the detection efficiency resulting in a smaller data set.

Figure 6 shows the ηn -invariant mass for $\gamma p \rightarrow \eta \pi^+ n$. Both decays of the η -meson were analyzed and are compared to each other by scaling the $\eta \rightarrow 3\pi^0$ results to the results of the $\eta \rightarrow 2\gamma$ data sample. Despite the lack of an individual efficiency correction, the overall features of the distributions are rather similar. Statistically significant finer structures are hard to identify due to the limited statistics. The main reasons for the worse statistical quality are the lower ($\sim 1/3$) detection efficiency for neutrons compared to protons and the fact that the experimental trigger required a high total energy (~ 550 MeV) deposited in the CB detector. Since neutrons deposit on average less energies than protons, and the π^+ does not contribute to the detected energy with its whole rest mass in contrast to the π^0 , the trigger is less efficient resulting in a smaller data set.

4.2 Enhancing a Potential $N(1685)$ -Signal

In order to enhance a possible signal of a narrow $N(1685)$ state, additional analysis cuts have to be applied. At the moment, only the $\gamma p \rightarrow \eta \pi^0 p$ reaction was studied regarding further cuts as statistics of the current $\gamma p \rightarrow \eta \pi^+ n$ data sample is too poor. This is expected to improve when all available data will have been analyzed.

In order to suppress contributions from the $\eta \Delta(1232)$ isobar, a cut requiring $m(\pi^0 p) < 1180$ MeV was applied. The resulting $m(\eta p)$ distributions are shown in figure 7. The data are again compared to a MC simulation weighted with the BnGa-model that was scaled to the data by the ratio of integrals. In bins two to four, the overall agreement is quite good considering the statistical uncertainties of both data and model. The statistical errors of the model are not shown directly but fluctuations are clearly visible. These fluctuations will be removed by generating a larger MC data sample in the final analysis. In the first bin, there are some noticeable deviations of the data from the model: For $m(\eta p) = 1640\text{--}1680$ MeV, the model seems to overestimate the data, which form a peak-like structure around 1690 MeV. The statistical significance of these features is low, though. Also, the scaling of the model to the data will need to be implemented using absolute normalizations in the final analysis rather than using a factor that averages over the whole distributions.

Figure 8 shows the $m(\eta p)$ distributions including the $m(\pi^0 p) < 1180$ MeV cut and requiring in addition that the event belongs to sector S5 in the Van Hove plot. As discussed in section 3.3, this is expected to be the predominant sector for the potential $\pi N(1685)$ isobar. Statistics

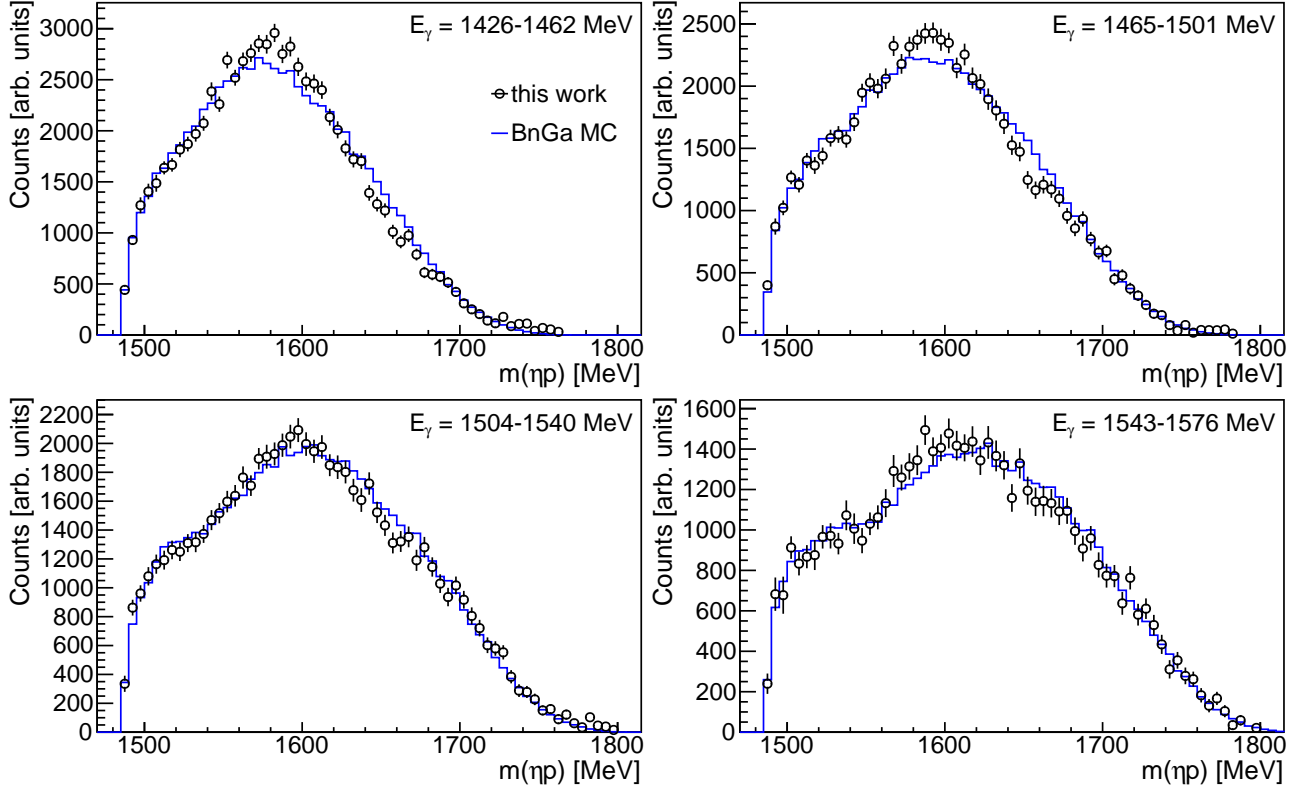


Figure 5. Invariant mass $m(\eta p)$ of $\gamma p \rightarrow \eta \pi^0 p$ for four bins of photon-beam energy (no acceptance correction). The data (black circles) are compared to a phase-space MC simulation (blue curves, normalized by integral ratio) using event weights from the BnGa partial-wave analysis of [45].

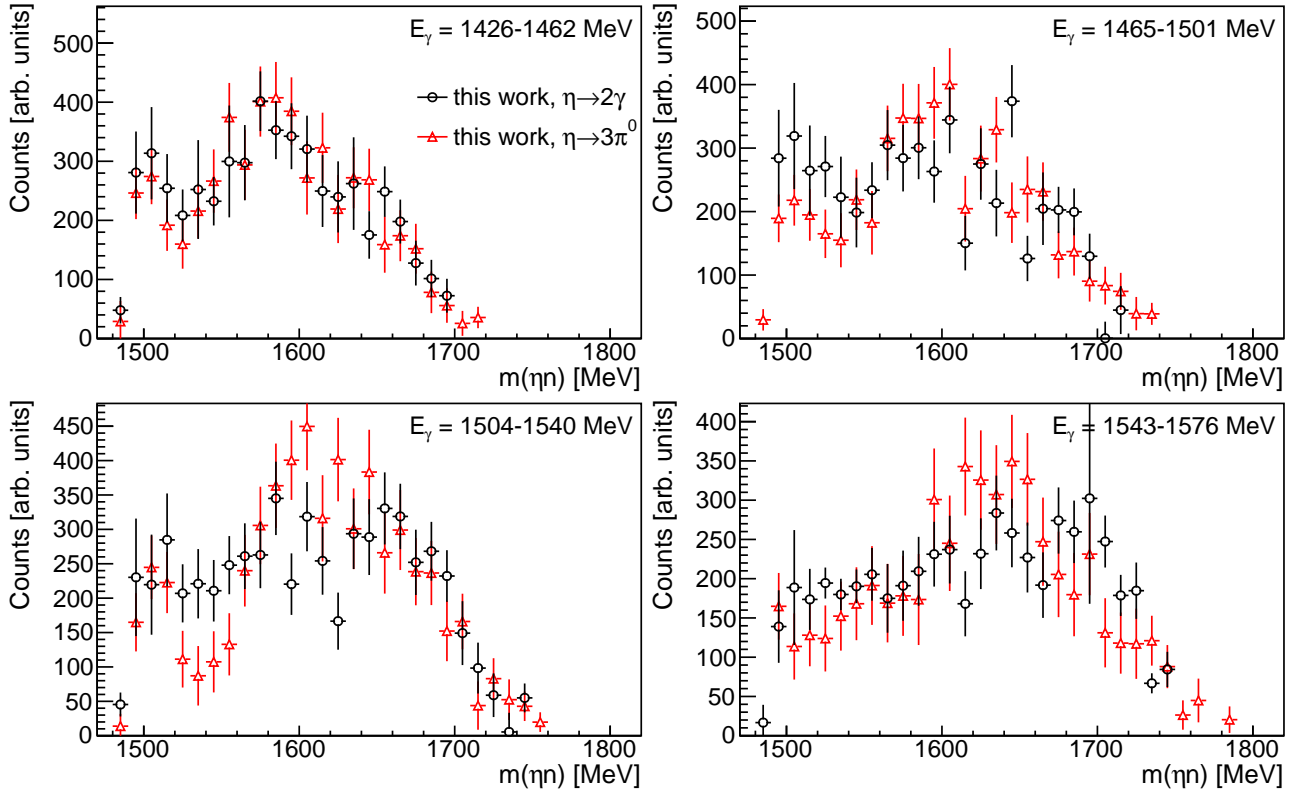


Figure 6. Invariant mass $m(\eta n)$ of $\gamma p \rightarrow \eta \pi^+ n$ for four bins of photon-beam energy (no acceptance correction). Two data samples using the $\eta \rightarrow 2\gamma$ decay (black circles) and the $\eta \rightarrow 3\pi^0$ decay (red triangles, normalized by integral ratio) have been analyzed.

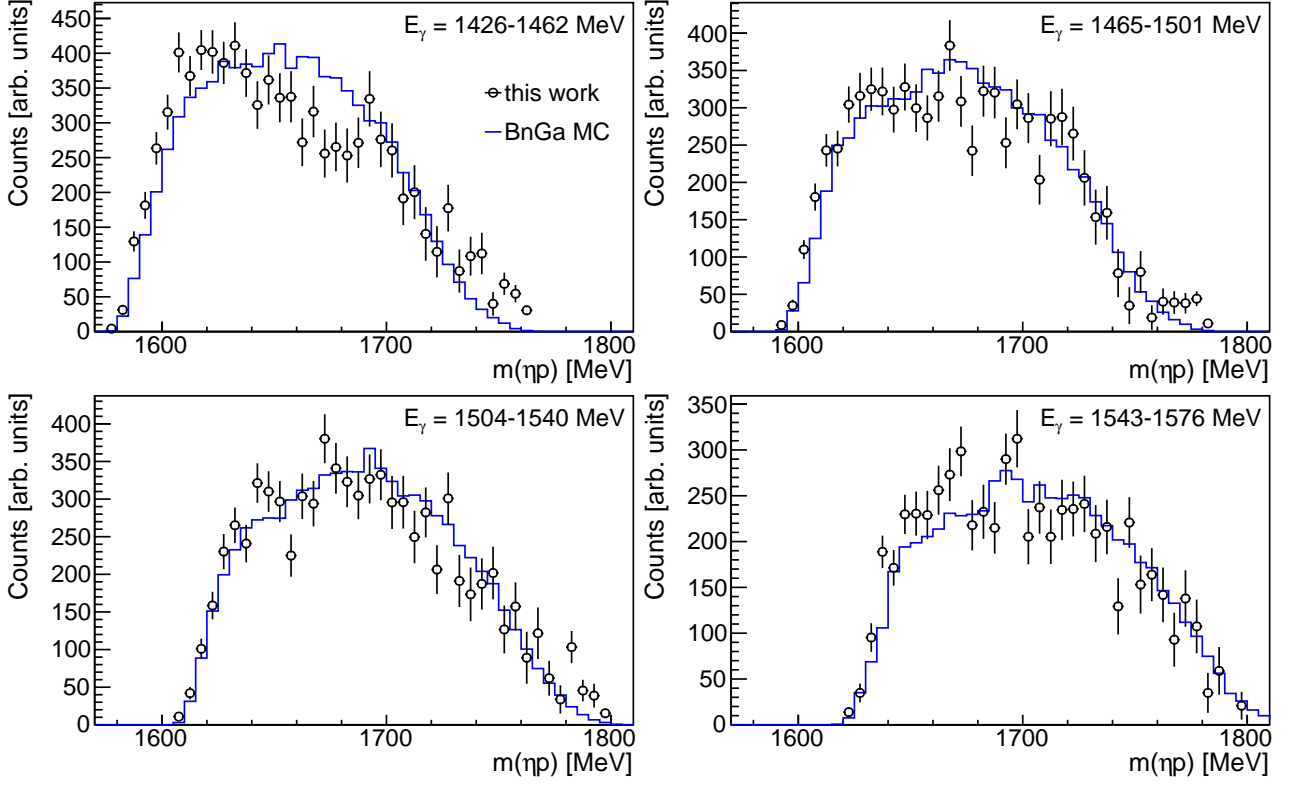


Figure 7. Invariant mass $m(\eta p)$ of $\gamma p \rightarrow \eta \pi^0 p$ for four bins of photon-beam energy with $m(\pi^0 p) < 1180$ MeV (no acceptance correction). The data (black circles) are compared to a phase-space MC simulation (blue curves, normalized by integral ratio) using event weights from the BnGa partial-wave analysis of [45].

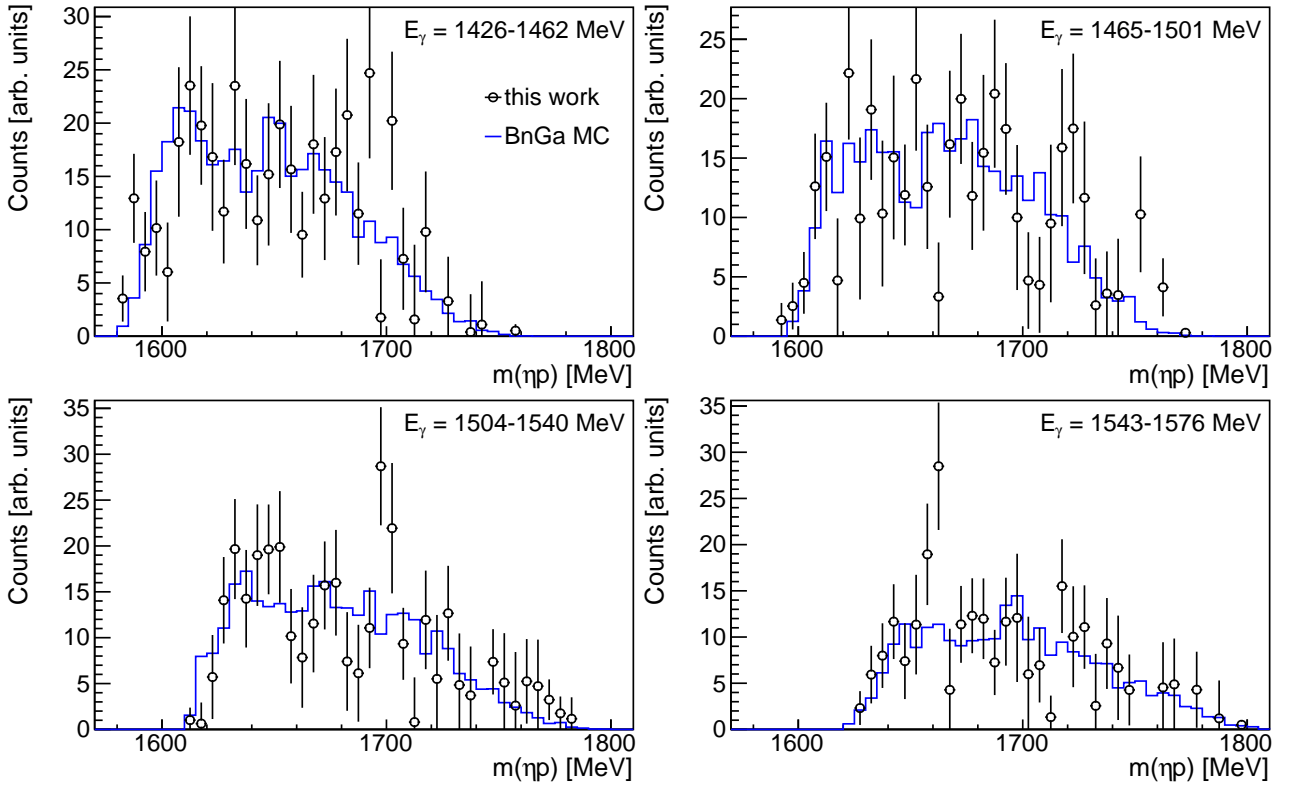


Figure 8. Invariant mass $m(\eta p)$ of $\gamma p \rightarrow \eta \pi^0 p$ for four bins of photon-beam energy with $m(\pi^0 p) < 1180$ MeV for events in the Van Hove plot-sector S5 (no acceptance correction). The data (black circles) are compared to a phase-space MC simulation (blue curves, normalized by integral ratio) using event weights from the BnGa partial-wave analysis of [45].

is obviously further reduced and fluctuations are also significant in the BnGa-model. Nevertheless, overall the data and model distribution agree rather well. Finer structures cannot be identified due to the limited statistics, although there a few bins with more entries around 1700 MeV, again not statistically significant.

5 Summary and Outlook

The reactions $\gamma p \rightarrow \eta\pi^0 p$ and $\gamma p \rightarrow \eta\pi^+ n$ in the energy range $E_\gamma=1.43\text{--}1.58$ GeV have been analyzed using data obtained at the A2 at MAMI experiment. The goal of this work was to check recent claims [40] of a signature of the $N(1685)$ -antidecuplet baryon in the $m(\eta p)$ and $m(\eta n)$ invariant masses of the reactions $\gamma N \rightarrow \eta\pi N$.

For $\gamma p \rightarrow \eta\pi^0 p$, our data show a good agreement with previous measurements represented by the BnGa partial-wave analysis [45]. When a cut requesting $m(\pi^0 p) < 1180$ MeV to suppress the dominating $\eta\Delta(1232)$ background is applied, there are some deviations between the data and the model around the region of interest for photon-beam energies $E_\gamma=1426\text{--}1462$ MeV. The statistical significance of these deviations is small, nevertheless this finding needs to be investigated further by increasing the statistical quality of both data and model. Having more data will also allow to get better statistics when using an additional cut on the preferred signal sector in the Van Hove plot, which could help isolating a small $\pi N(1685)$ contribution to the reaction.

The $\gamma p \rightarrow \eta\pi^+ n$ analysis currently lacks the statistical quality for a refined analysis regarding a narrow $N(1685)$. All of the available data need to be analyzed in combination with an optimized event selection to come to a final conclusion here.

Next steps will include optimizations in the analysis ($\eta \rightarrow 3\pi^0$ decay for $\eta\pi^0 p$ final state, cuts, test of inclusive analyses), the use of all available data, the generation of a larger MC data sample using the BnGa-model, and acceptance correction with absolute normalization and comparison with the Mainz model [50].

References

- [1] R. Aaij et al., Phys. Rev. Lett. **115**, 072001 (2015)
- [2] R. Aaij et al., Phys. Rev. Lett. **122**, 222001 (2019)
- [3] A. Ali et al., Phys. Rev. Lett. **123**, 072001 (2019)
- [4] D. Winney et al., Phys. Rev. D **100**, 034019 (2019)
- [5] T. Nakano et al., Phys. Rev. Lett. **91**, 012002 (2003)
- [6] K.H. Hicks, Eur. Phys. J. H **37**, 1 (2012)
- [7] M. Yosoi, EPJ Web Conf. **199**, 01020 (2019)
- [8] V.V. Barmin et al., Phys. Rev. C **89**, 045204 (2014)
- [9] M.J. Amarian et al., Phys. Rev. C **85**, 035209 (2012)
- [10] R.L. Jaffe, Topical Conference on Baryon Resonances, Oxford, SLAC-PUB-1774 (1976)
- [11] H. Högaasen, P. Sorba, Nucl. Phys. B **145**, 119 (1978)
- [12] D. Diakonov, V. Petrov, M. Polyakov, Z. Phys. A **359**, 305 (1997)
- [13] V. Kuznetsov et al., Phys. Lett. B **647**, 23 (2007)
- [14] R.A. Arndt et al., Phys. Rev. C **69**, 035208 (2004)
- [15] M.V. Polyakov, A. Rathke, Eur. Phys. J. A **18**, 691 (2003)
- [16] F. Miyahara et al., Prog. Theor. Phys. Suppl. **168**, 90 (2007)
- [17] I. Jaegle et al., Phys. Rev. Lett. **100**, 252002 (2008)
- [18] I. Jaegle et al., Eur. Phys. J. A **47**, 89 (2011)
- [19] D. Werthmüller et al., Phys. Rev. Lett. **111**, 232001 (2013)
- [20] D. Werthmüller et al., Phys. Rev. C **90**, 015205 (2014)
- [21] L. Witthauer et al., Eur. Phys. J. A **49**, 154 (2013)
- [22] V. Kuznetsov et al., Acta Phys. Polon. B **39**, 1949 (2008)
- [23] V. Kuznetsov et al., Phys. Rev. C **83**, 022201 (2011)
- [24] V. Kuznetsov et al., Phys. Rev. C **91**, 042201 (2015)
- [25] K.S. Choi et al., Phys. Lett. B **636**, 253 (2006)
- [26] A. Fix, L. Tiator, M.V. Polyakov, Eur. Phys. J. A **32**, 311 (2007)
- [27] A.V. Anisovich et al., Eur. Phys. J. A **41**, 13 (2009)
- [28] M. Shrestha, D.M. Manley, Phys. Rev. C **86**, 055203 (2012)
- [29] J. Beringer et al. (Particle Data Group), Phys. Rev. D **86**, 010001 (2012)
- [30] V. Shklyar, H. Lenske, U. Mosel, Phys. Lett. B **650**, 172 (2007)
- [31] R. Shyam, O. Scholten, Phys. Rev. C **78**, 065201 (2008)
- [32] M. Döring, K. Nakayama, Phys. Lett. B **683**, 145 (2010)
- [33] L. Tiator et al., EPJ Web Conf. **199**, 01019 (2019)
- [34] A.V. Anisovich et al., Eur. Phys. J. A **49**, 67 (2013)
- [35] A.V. Anisovich et al., Eur. Phys. J. A **51**, 72 (2015)
- [36] L. Witthauer et al., Phys. Rev. Lett. **117**, 132502 (2016)
- [37] L. Witthauer et al., Eur. Phys. J. A **53**, 58 (2017)
- [38] L. Witthauer et al., Phys. Rev. C **95**, 055201 (2017)
- [39] A.V. Anisovich et al., Phys. Rev. C **95**, 035211 (2017)
- [40] V. Kuznetsov et al., JETP Letters **106**, 693 (2017)
- [41] T. Nakabayashi et al., Phys. Rev. C **74**, 035202 (2006)
- [42] J. Ajaka et al., Phys. Rev. Lett. **100**, 052003 (2008)
- [43] I. Horn et al., Eur. Phys. J. A **38**, 173 (2008)
- [44] E. Gutz et al., Phys. Lett. B **687**, 11 (2010)
- [45] E. Gutz et al., Eur. Phys. J. A **50**, 74 (2014)
- [46] V.L. Kashevarov et al., Eur. Phys. J. A **42**, 141 (2009)
- [47] V.L. Kashevarov et al., Phys. Lett. B **693**, 551 (2010)
- [48] J.R.M. Annand et al., Phys. Rev. C **91**, 055208 (2015)
- [49] A. Käser et al., Eur. Phys. J. A **52**, 272 (2016)
- [50] V. Sokhoyan et al., Phys. Rev. C **97**, 055212 (2018)
- [51] P. Adlarson et al., Phys. Rev. C **92**, 024617 (2015)
- [52] S. Agostinelli et al., Nucl. Instrum. Methods Phys. Res., Sect. A **506**, 250 (2003)

[53] M. Pivk, F.R. Le Diberder, Nucl. Instrum. Methods
Phys. Res., Sect. A **555**, 356 (2005)

[54] L. Van Hove, Nucl. Phys. B **9**, 331 (1969)